Intra-uterine tissue engineering of full-thickness skin defects in a fetal sheep model

Hosper, Nynke A.; Eggink, Alex J.; Roelofs, Luc A. J.; Wijnen, Rene M. H.; van Luyn, Marja J. A.; Bank, Ruud A.; Harmsen, Martin C.; Geutjes, Paul J.; Daamen, Willeke F.; van Kuppevelt, Toin H.

Published in:
Biomaterials

DOI:
10.1016/j.biomaterials.2010.01.129

Publication date:
2010

Biomaterials 31 (2010) 3910–3919

Contents lists available at ScienceDirect

Biomaterials

journal homepage: www.elsevier.com/locate/biomaterials

Intra-uterine tissue engineering of full-thickness skin defects in a fetal sheep model

Nynke A. Hosper [a,*,1], Alex J. Eggink [b,1], Luc A.J. Roelofs [c], Rene M.H. Wijnen [d], Marja J.A. van Luyn [a], Ruud A. Bank [a], Martin C. Harmsen [a], Paul J. Geutjes [c], Willeke F. Daamen [e], Toin H. van Kuppevelt [e], Dorien M. Tiemessen [c], Egbert Oosterwijk [c], Jane J. Crevels [f], Willeke A.M. Blokx [g], Fred K. Lotgering [b], Paul P. van den Berg [f], Wout F.J. Feitz [c]

[a] University Medical Center Groningen, University of Groningen, Department of Pathology and Medical Biology, Hanzeplein 1, EA11, 9713 GZ Groningen, The Netherlands
[b] Department of Obstetrics and Gynecology, Radboud University Nijmegen Medical Centre, 6500 HB Nijmegen, The Netherlands
[c] Department of Urology, Radboud University Nijmegen Medical Centre, 6500 HB Nijmegen, The Netherlands
[d] Department of Pediatric Surgery, Radboud University Nijmegen Medical Centre, 6500 HB Nijmegen, The Netherlands
[e] Department of Biochemistry, NCMLS, Radboud University Nijmegen Medical Centre, 6500 HB Nijmegen, The Netherlands
[f] Department of Obstetrics and Gynecology, University Medical Centre Groningen, 9713 GZ Groningen, The Netherlands
[g] Department of Pathology, Radboud University Nijmegen Medical Centre, 6500 HB Nijmegen, The Netherlands

ARTICLE INFO

Article history:
Received 22 December 2009
Accepted 19 January 2010
Available online 18 February 2010

Keywords:
Spina bifida
Fetal wound healing
Intra-uterine repair
Collagen scaffold
Vascular endothelial growth factor
Basic fibroblast growth factor

ABSTRACT

In spina bifida the neural tube fails to close during the embryonic period and it is thought that prolonged exposure of the unprotected spinal cord to the amniotic fluid during pregnancy causes additional neural damage. Intra-uterine repair might protect the neural tissue from exposure to amniotic fluid and might reduce additional neural damage. Biodegradable collagen scaffolds may be useful in case of fetal therapy for spina bifida, but biochemical properties need to be studied. The aim of this study was to investigate whether biodegradable collagen scaffolds can be used to treat full-thickness fetal skin defects. We hypothesized that the pro-angiogenic growth factors VEGF and FGF2 would enhance vascularization, epidermialization and lead to improved wound healing. To investigate the effect of these two growth factors, a fetal sheep model for skin defects was used. Compared to wounds treated with bare collagen scaffolds, wounds treated with growth factor-loaded scaffolds showed excessive formation of capillaries and less myofibroblasts were present in these wounds, leading to less contraction. This study has demonstrated that collagen scaffolds can be used to treat fetal skin defects and that the combination of collagen scaffolds with VEGF and FGF2 had a beneficial effect on wound healing.

1. Introduction

There are different congenital structural anomalies in which closure of skin and underlying structures does not occur during embryonic development. In spina bifida (incidence rate 1 of every 2000 live births) the neural tube fails to close during the embryonic period and it is thought that exposure of the neural tube to the amniotic fluid during pregnancy causes additional neural damage (second hit hypothesis) [1]. Current treatment of spina bifida consists of surgical closure of the defect in the early postnatal period, in order to prevent infection and further damage. However, the damage caused by the exposure to the amniotic fluid is irreversible.

It is expected that intra-uterine repair of the defect diminishes the damage caused by exposure to amniotic fluid. An additional advantage of such a fetal intervention is that fetal tissue can regenerate, instead of repair with fibrosis [2]. During the first and second trimester of development, fetal skin wounds heal with a normal epidermal and dermal architecture. During the third trimester a transition from scarless repair to fibrotic repair occurs, which is comparable to adult wound healing with more inflammation and fibrosis [2]. However, the ability of the fetus to heal full-thickness wounds without fibrosis depends on the size of the defect, independent of the gestational age [3].

The aim of this study was to investigate whether biodegradable collagen scaffolds can be used to treat full-thickness fetal skin defects to allow *in situ* fetal dermal repair and epidermal overgrowth. For this purpose we developed a fetal skin defect model in sheep, and treated the defects with a cross-linked type I collagen

* Corresponding author. Tel.: +31 50 3615180; fax: +31 50 3619911.
E-mail address: n.a.hosper@med.umcg.nl (N.A. Hosper).
[1] These authors contributed equally to this study.

0142-9612/$ – see front matter © 2010 Elsevier Ltd. All rights reserved.
doi:10.1016/j.biomaterials.2010.01.129

scaffold (which was previously applied in a rat model and sheep model [4–7]). Collagen scaffolds can be modulated in different ways to enhance and regulate wound healing. The porous matrix structure can be varied and growth factors can be incorporated to promote angiogenesis and cellular ingrowth. In this study we used a collagen scaffold and a collagen scaffold loaded with heparin and two growth factors: vascular endothelial growth factor (VEGF) and basic fibroblast growth factor (FGF2). Heparin was used for optimal growth factor binding. VEGF is a 40–45-kDa homodimeric glycoprotein promoting angiogenesis [8]. FGF2 can also act as angiogenic factor by directing endothelial cell migration and proliferation. The combination of VEGF and FGF2 has been reported to have potent synergistic effects on neovascularization both in *in vitro* and *in vivo* experiments [9–12]. Furthermore, FGF2 reduces scar formation when exogenously applied to the wound site [13] and diminishes wound contraction, when used in combination with a collagen matrix [14]. FGF2 can also act as a potent mitogen for fibroblasts and keratinocytes [15,16], indicating an effect on both dermal as well as epidermal healing. With the stimulation of vascular ingrowth and cellular infiltration, regeneration of tissue can be improved by supplying sufficient oxygen and nutrients. By regulating the host response to the scaffold in this way, formation of excess scar formation may be prevented.

We evaluated fetal wound healing and closure of full-thickness skin wounds by means of intra-uterine tissue engineering using type I collagen scaffolds (COL) and heparinised type I collagen scaffolds loaded with VEGF and FGF2 (COL-HEP/VF), and compared these with untreated defects 2, 4 and 8 weeks after fetal surgery. Cellular ingrowth, vascularization, scar tissue formation and degradation of the scaffolds were evaluated by histology and immunohistochemistry.

2. Materials and methods

The study has been approved by the local Ethics Committee on Animal Research of the Radboud University Nijmegen, The Netherlands (RU-DEC 2007-239).

2.1. Preparation of collagen scaffolds

Type I collagen was purified from bovine achilles tendon as described previously [17,18]. To prepare collagen scaffolds, a 0.67% (w/v) type I collagen suspension in 0.25 M acetic acid was shaken overnight at 4 °C and homogenized on ice using a Potter–Elvehjem homogenizer (Louwers Glass and Ceramic Technologies, Hapert, The Netherlands). Air bubbles were removed by centrifugation at 100*g* for 15 min at 4 °C. The suspension was then poured into 6-well plates (4 mL per well), frozen at −20 °C, and lyophilized. Scaffolds were pre-incubated with 50 mM 2-morpholinoethane sulfonic acid (MES) pH 5.0 containing 40% ethanol for 30 min at 22 °C. After removal of this solution, scaffolds were cross-linked using 33 mM 1-ethyl-3-(3-dimethyl aminopropyl) carbodiimide (EDC) and 6 mM *N*-hydroxysuccinimide (NHS) in 50 mM MES pH 5.0 containing 40% ethanol for 4 h at 22 °C in the presence or absence of 0.25% heparin (Diosynth, Oss, The Netherlands). Scaffolds were then washed, frozen and lyophilized. Scaffolds were disinfected in 70% ethanol (6 × 7 mL per well) followed by washings with sterile PBS (8 × 7 mL per well). The cross-linked type I collagen scaffold is abbreviated in the text as COL.

The growth factors vascular endothelial growth factor 165 (VEGF; human recombinant, R&D Systems, Minneapolis, MN, USA) and basic fibroblast growth factor 2 (FGF2; human recombinant, R&D Systems) were loaded onto the heparin-cross-linked collagen scaffolds by incubating six Ø 12 mm scaffolds in 5 mL PBS containing 3.5 μg/mL VEGF and 3.5 μg/mL FGF2, followed by 3 washings with the same volume of PBS. This scaffold is abbreviated in the text as COL-HEP/VF.

2.2. Analysis of collagen scaffolds

The ultrastructure of the scaffolds was visualized by scanning electron microscopy (SEM). Specimens were mounted on stubs, sputtered with an ultrathin layer of gold in a Polaron E5100 coating system and visualized with a JEOL JSM-6310 SEM apparatus operating at 15 kV.

The degree of cross-linking of the scaffolds was determined spectrophotometrically by determining the amine group content using 2,4,6-trinitrobenzene sulfonic acid. Cross-linking efficiency was expressed as the percentage of the total number of amine groups that were used in the cross-linking process [19,20].

The heparin content of the films was determined applying a hexosamine assay using *p*-dimethylamino-benzaldehyde, taking heparin as a standard [21,22].

The amount of growth factors bound to the scaffolds was determined with sodium dodecyl sulfate polyacrylamide gel electrophoresis (SDS-PAGE) on a 15% (w/v) gel, followed by silver staining using a 0.1% (w/v) $AgNO_3$ solution. COL-HEP scaffolds incubated with growth factors and a standard curve of 0–100 ng of either VEGF of FGF2 were incubated for 15 min in a boiling water bath under reducing conditions using 5% (v/v) 2-mercaptoethanol. The intensity of the bands was analyzed using Adobe Photoshop.

The location of growth factors in the scaffolds was visualized by immunohistochemistry using the ABC method [23] with antibodies HS4C3 [24], goat-anti-human VEGF (Sigma Chemical Co., St Louis, MO, USA) and rabbit-anti-bovine FGF2 (R&D Systems, Minneapolis, MN, USA).

2.3. Animals and surgical procedures

Nine pregnant ewes of Dutch Texel breed underwent surgery at 79 days' gestation (term, 140–147 days). For sedation, the animals were pre-medicated with an intramuscular injection of midazolam (0.5 mg/kg). Anesthesia for surgery was induced by an intravenous injection of propofol (5 mg/kg) followed by tracheal intubation. The ewes were maintained on general anesthesia with 1.5% isoflurane. For analgesia, flunixin (2 mg/kg) and sufentanil (4 μg/kg) were given intravenously followed by a maintenance dosage sufentanil of 2 μg/kg/h. Heart rate, temperature, oxygen saturation and carbon dioxide concentration of the expired air were monitored. Fetal anesthesia was achieved by transplacental passage of the medications, administered to the ewe. The abdomen was shaved, cleaned and aseptically prepared. After a low midline laparotomy under sterile conditions, the uterus was inspected for the number of fetuses. One uterus horn was exteriorized, wrapped in gauzes soaked with warm phosphate buffered saline (PBS), and the position of the fetal lamb was determined by palpation. At a favorable location over the caudal side of the fetus a hysterotomy was made.

Three circular skin lesions, 12 mm in diameter, were made on the back of the fetus by excising the skin. The lesion on the left side was covered with a collagen scaffold (COL). The lesion on the right side was covered with the collagen–heparin scaffold with VEGF and FGF2 (COL-HEP/VF). The applied scaffolds were slightly thicker than the removed skin. The lesion in the middle of the back remained uncovered. The scaffolds were secured and marked with four 6-0 prolene (Ethicon, Somerville, NJ, USA) interrupted sutures around the skin lesion. After surgery the fetus was replaced in the uterus and the amniotic fluid volume was restored with warm PBS solution. Amoxicillin (250 mg) was added to the amniotic fluid. The uterus was closed with a running suture in 2 layers using 2-0 vicryl (Ethicon, Somerville, NJ, USA). In case of twin pregnancy the same procedure was performed using the techniques as described above. Sodium penicillin (1,000,000 IU) was administered to the intra-abdominal space and the abdominal wall was closed in 3 layers using EP6 Serafil for the fascia, 2-0 Vicryl for the subcutaneous tissue and 1-0 Vicryl Plus for the skin. Depomycin (20,000 IU penicillin ml^{-1}, 200 mg streptomycin ml^{-1}) was initiated preoperatively (0.6 ml/10 kg) and maintained postoperatively (1 ml/10 kg) for 3 days via intramuscular injections. Buprenorphine (10 μg/kg, intravenous) and flunixin (2 mg/kg, intramuscular) were given for three days to provide postoperative analgesia. The ewes returned to the farm soon after they were able to stand.

2.4. Macroscopic evaluation

The animals were sacrificed at three time points. Evaluation took place at 93 days' gestation (2 weeks post surgery), 107 days' gestation (4 weeks post surgery) and 140 days' gestation (term) in group 1, 2 and 3 respectively. Ewes and fetal lambs were euthanized by 10 mL intravenously and 5 mL intracardiacally injected T61® (200 mg embutramide ml^{-1}, 50 mg mebezoniumjodide ml^{-1} and 5 mg tetracainhydrochloride ml^{-1}; Intervet, Boxmeer, The Netherlands).

After macroscopic evaluation and photography of the wound, the size of the defect was measured between the marking sutures and was used to calculate wound contraction. Wound contraction was expressed as the percentage of the size of the defect at time of evaluation against the original size of the defect of 12 mm at time of surgery. All data are represented as mean ± SEM. The data were analyzed using computer statistical software (GraphPad Prism, GraphPad Software Inc.). The statistic significance of differences in the findings was evaluated by a one-way ANOVA followed by post hoc Bonferroni analysis. A difference was considered statistically significant when $p < 0.05$.

2.5. Histological techniques

Samples of the skin and subcutaneous tissue were taken at the level of the skin lesions, fixed in 4% (v/v) buffered formaldehyde and paraffin-embedded for histological analysis or snap-frozen and stored at −80 °C. Serial cross-sections were cut (4 μm) and stained with haematoxylin and eosin, toluidine blue and Masson's trichrome. Additionally, immunohistochemical stainings for α-smooth muscle actin (α-SMA), pancytokeratin and type IV collagen were performed on paraffin-embedded sections. The sections were deparaffinized and washed with PBS. Endogenous peroxidases were blocked with 3% (v/v) H_2O_2/PBS for 30 min at room

temperature. Heat mediated antigen retrieval in Sodium Citrate Buffer (10 mM Sodium Citrate, pH 6.0) during 10 min was performed for sections stained for α-SMA and cytokeratin. Sections stained with anti-type IV collagen were treated with 0.1% (v/v) protease (Sigma–Aldrich, St. Louis, MO, USA) for 30 min at room temperature for antigen retrieval. Slides were pre-incubated with 5% serum from the species that produced the secondary antibody.

α-SMA was detected with mouse α-SMA (1:15.000, clone 1A4; Sigma–Aldrich) and peroxidase-conjugated goat-anti-mouse antibody (1:200; SBA, Birmingham, USA, cat.no.1080-05). Immunostaining of cytokeratin was performed by overnight incubation at 4 °C of mouse-anti-cytokeratin (1:800, clone AE1/AE3; Labvision corporation, Fremont, USA), followed by biotinylated horse-anti-mouse and peroxidase-conjugated ABC complex (Vector Laboratories, Burlingame, USA). Type IV collagen was detected using rabbit anti-type IV collagen (1:100; Abcam, Cambridge, UK), biotinylated goat-anti-rabbit (Dako) and peroxidase–conjugated streptavidine (Dako). Color development was performed with power DAB (α-SMA and cytokeratin, Immunologic, Duiven, The Netherlands,) and 3-amino-9-ethylcarbazole (type IV collagen, Sigma, Steinheim, Germany). Sections were counterstained with Mayer's haematoxylin (Fluka Chemie, Buchs, Switzerland).

3. Results

3.1. Scaffolds

Scanning electron microscopy revealed a porous scaffold with a rather open top side and a more closed pan side (Fig. 1A). Cross-linking efficiency was 31 ± 8% for COL scaffolds and 31 ± 4% for heparinised COL scaffolds (mean ± SD). To heparinised COL scaffolds, 13.1 ± 2.4% heparin was bound (mean ± SD). Heparin was bound evenly throughout the scaffold. The amount of growth factors bound per mg heparinised COL scaffold was 0.26 ± 0.05 μg for VEGF and 0.10 ± 0.04 μg (mean ± SD) for FGF2. FGF2 was present throughout the scaffold whereas VEGF was mainly present at the edges of the scaffold (Fig. 1B).

3.2. Animal surgery

Eight ewes and 13 fetal lambs underwent surgery (6 ewes were bearing twins). The overall fetal survival rate was 85% during the pregnancy period. In one sheep, twin pregnancy could not be determined at time of surgery and only one fetus was operated. One sheep aborted 2 days after the surgery probably due to severe enteritis of the ewe and needed to be sacrificed accounting for the only maternal death in the study. At autopsy, herniation of a bowel loop between the fascial sutures was found. In one sheep, a thermal intestinal lesion occurred during the surgery which was repaired. All other procedures went uneventful. Eleven lambs were evaluated; four in group 1 (93 days), three in group 2 (107 days) and four in group 3 (140 days). The survival rate was similar to previously published data for fetal surgery on similarly aged fetal lambs [5–7].

3.3. Macroscopic evaluation

A macroscopic overview with examples of wound healing is depicted in Fig. 2A. On macroscopic inspection, the skin defects

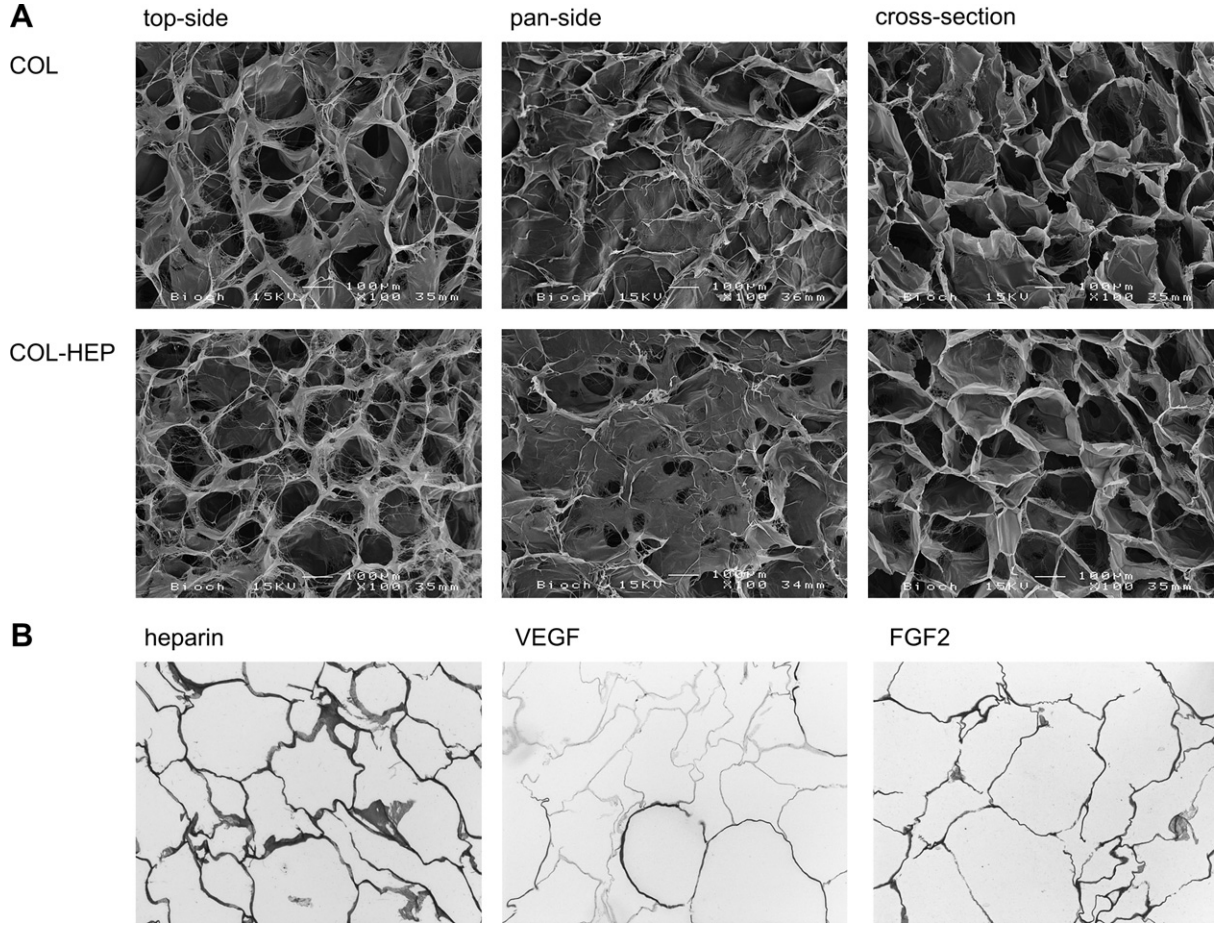

Fig. 1. Scanning electron microscopical images of collagen scaffolds cross-linked in the absence (top row) or presence of heparin (bottom row) (A). Shown are the top view, bottom view and cross-section. The more closed pan side was implanted such that it was in contact with the amniotic fluid. Immunolocalisation of heparin, VEGF and FGF2 in the COL-HEP/VF scaffolds (B). Note that heparin and FGF2 were evenly distributed through the scaffold, while VEGF was mainly found at the edge of the scaffold.

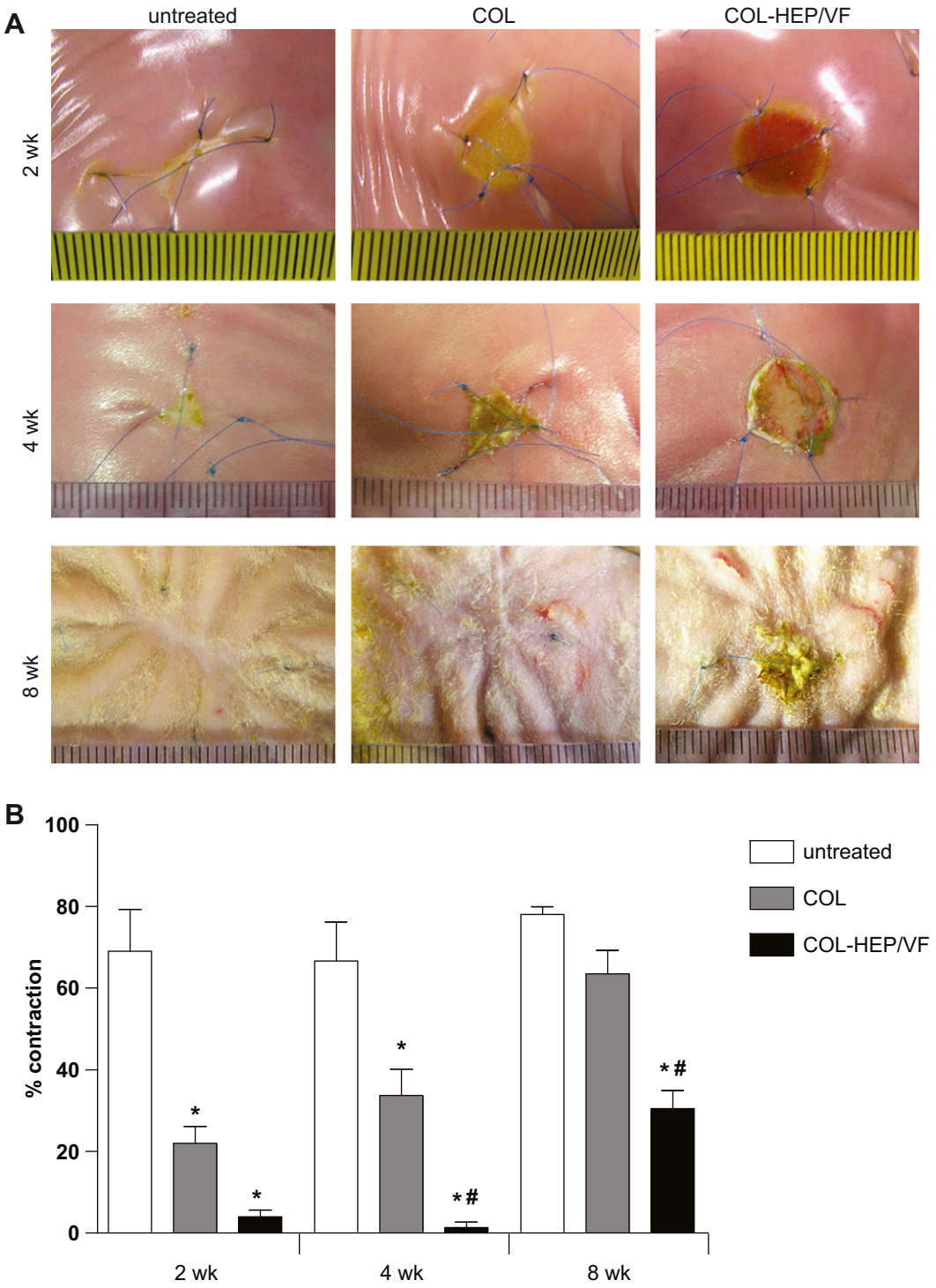

Fig. 2. Macroscopical overview of wound healing after surgery at 93 days' (2 weeks post surgery), 107 days' (4 weeks post surgery) and 140 days' gestation (term) (A). Note the shape of contraction of the untreated lesion and the reddish appearance of the wound treated with COL-HEP/VF. Percentage of wound contraction (B). At 2 and 4 weeks post surgery less contraction was present in COL treated wounds compared to untreated wounds. At all time points less contraction was present in COL-HEP/VF treated wounds compared to untreated wounds. * significant difference between untreated and COL or COL-HEP/VF ($p < 0.05$). # significant difference between COL and COL-HEP/VF treated ($p < 0.05$).

were visible in all groups. The untreated defects were completely closed at 8 weeks post surgery, with the wound edges contracted to each other. COL treated wounds showed remnants of the scaffold at 2 and 4 weeks post surgery, at term (8 weeks post surgery) the wound was completely closed without visible remnants of the scaffold. A reddish appearance of the remnants of the COL-HEP/VF treated wounds was present at 2 weeks, suggesting angiogenesis. In contrast to COL treated wounds, COL-HEP/VF treated wounds showed remnants of the scaffold at term.

The percentage of wound contraction of the treated and untreated defects is shown in Fig. 2B. At 2 weeks, the percentage of wound contraction of the COL treated defects was decreased and this was more obvious when using a COL-HEP/VF scaffold. At 4 and 8 weeks, contraction was also found in the COL treated defects but

again the contraction of the COL-HEP/VF scaffold was less (~30%). At term, the degree of wound contraction of the uncovered group was almost 80%.

3.4. Microscopic evaluation

Two weeks after surgery (93 days' gestation), the *untreated wounds* were covered by a fibrin clot. The newly formed epidermis fully closed the wound area and separated the granulation tissue from the clot; the epidermal cells had migrated over the interface between the clot and the developing granulation tissue. The newly formed epidermis was, at this time point, less than twice as thick as the normal epidermis distal from the wound area (Fig. 3A); the overall thickness was very regular (Fig. 4A). The granulation tissue consisted of a more open extracellular matrix (ECM) network compared to the normal dermis and was populated by numerous cells (Fig. 3A2). The latter appeared to be mainly myofibroblasts as based on their morphology and confirmed by α-SMA staining (Fig. 5A). Compared to the normal fetal dermis in development, less mature blood vessels and capillaries were present in the wounded area (Fig. 3A).

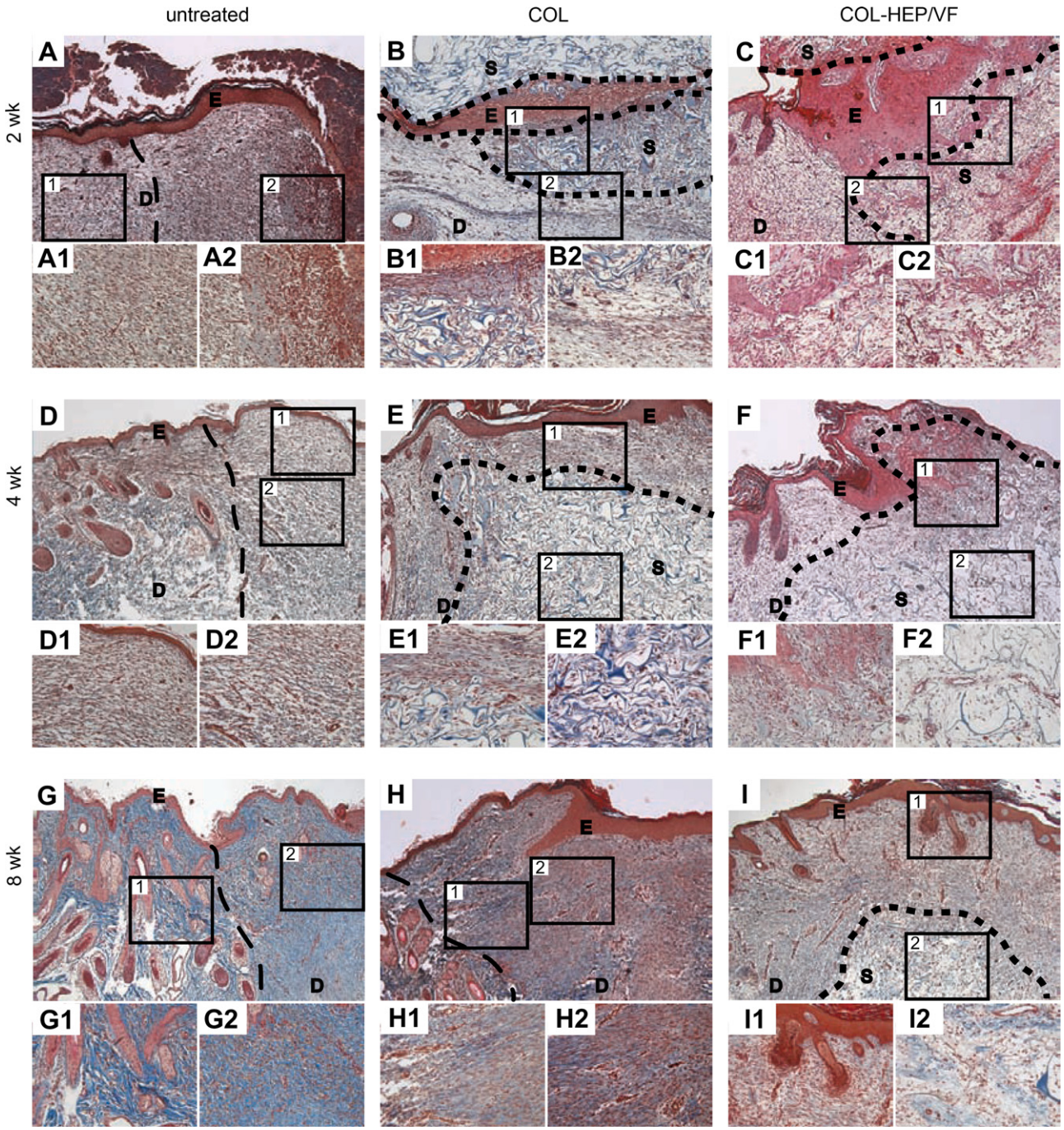

Fig. 3. Masson's trichrome staining of skin defects at different time points. Untreated defect at 2 weeks (A), 4 weeks (D) and 8 weeks (G). Defect treated with COL at 2 weeks (B), 4 weeks (E) and 8 weeks (H). Defect treated with COL-HEP/VF at 2 weeks (C), 4 weeks (F) and 8 weeks (I). The black striped line indicates the edge of the defect; the black dotted line indicates the border between surrounding tissue and the scaffold. E = epidermis, D = dermis, S = scaffold. The boxed areas denote the corresponding region of higher magnification images. Original magnifications: 50× (A–I) and 200× (A1–I1).

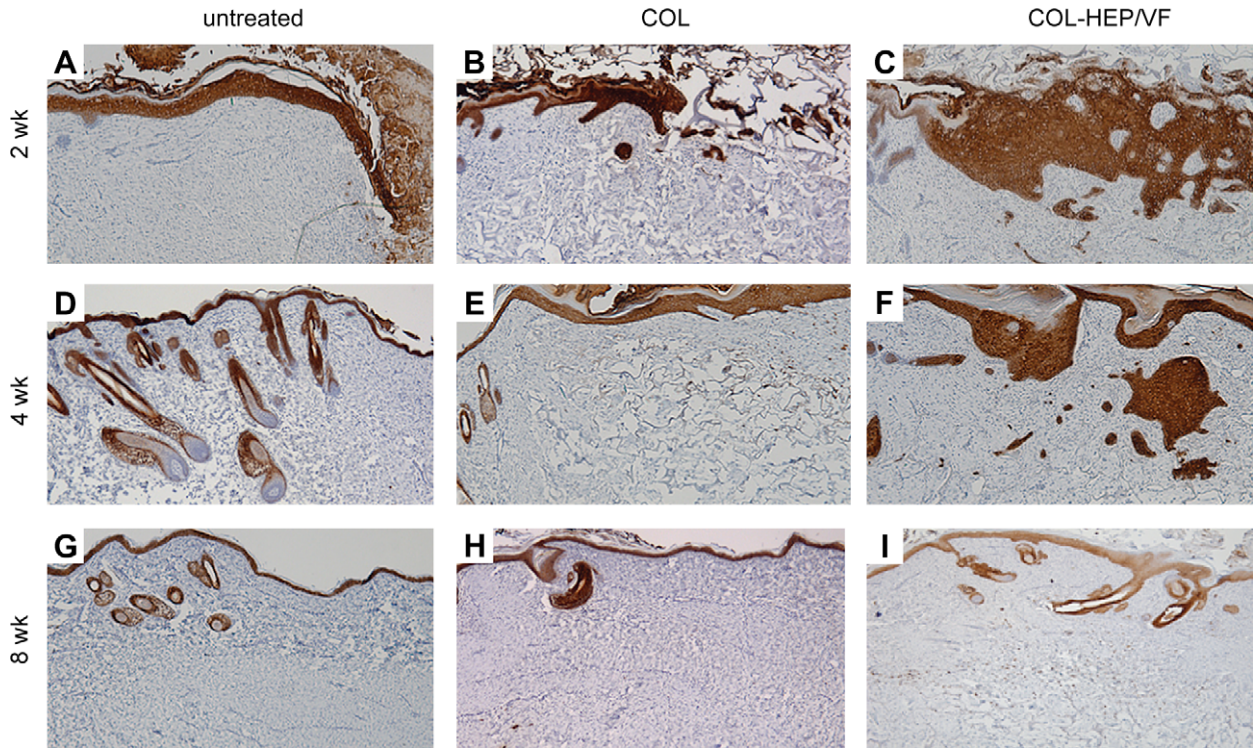

Fig. 4. Epithelialization. Cytokeratin staining of skin defects at different time points. Untreated defect at 2 weeks (A), 4 weeks (D) and 8 weeks (G). Defect treated with COL at 2 weeks (B), 4 weeks (E) and 8 weeks (H). Defect treated with COL-HEP/VF at 2 weeks (C), 4 weeks (F) and 8 weeks (I). Original magnifications: 50× (A–I).

The wounds treated with the COL scaffold showed a fibrin clot covering the top of the scaffold (not shown). Interestingly, the epidermis grew from both sides through the upper part of the scaffold, but did not completely close at this time point. The thickness and shape of the newly formed epidermis was rather irregular (Figs. 3B and 4B) and was generally thicker than the epidermis of the untreated wound (i.e. the wound without a scaffold). New ECM formation occurred at the interface between the

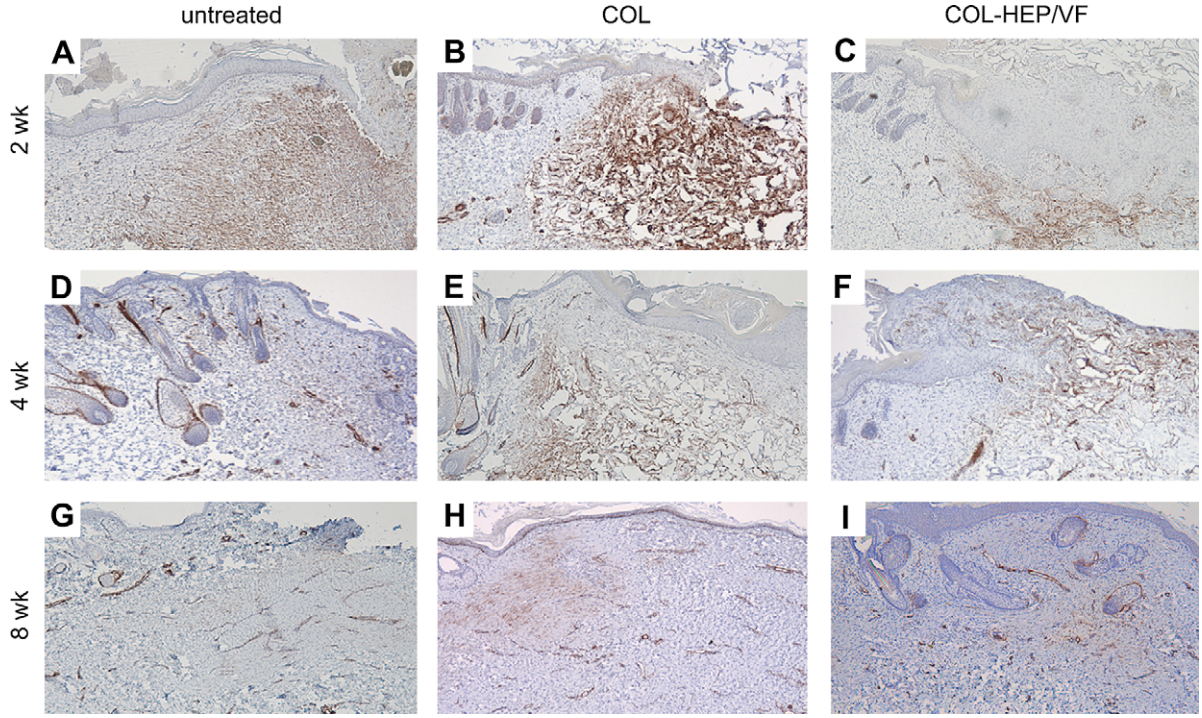

Fig. 5. Myofibroblasts. SMA staining of skin defects at different time points. Untreated defect at 2 weeks (A), 4 weeks (D) and 8 weeks (G). Defect treated with COL at 2 weeks (B), 4 weeks (E) and 8 weeks (H). Defect treated with COL-HEP/VF at 2 weeks (C), 4 weeks (F) and 8 weeks (I). Original magnifications: 50× (A–I).

scaffold and the epidermis (Fig. 3B1), whereas less ECM formation was observed at the dermal side of the scaffold (Fig. 3B2). Infiltration of cells, mainly α-SMA positive (Fig. 5B), was seen in the scaffold. In the scaffold only a few small blood vessels were formed (Fig. 3B).

The wounds treated with the COL-HEP/VF scaffold also showed a fibrinous clot on top of the scaffold. Here again, the epidermis grew from both sides through the upper part of the scaffold. However, the newly formed epidermis was much more hyperplastic (Fig. 3C versus B; Fig. 4C versus B) with a highly irregular shape. The wound area was also not completely covered by the epidermis. Less ECM formation was seen at the interface between the scaffold and the epidermis compared to the wound treated with the bare COL implant (Fig. 3C1 versus B1; Fig. 3C2 versus B2) and fewer α-SMA-positive cells infiltrated into the scaffold (Fig. 5C versus B). A few small blood vessels were present in the scaffold (Fig. 3C), which was comparable to the amount in the COL treated wound at this time point.

Four weeks after surgery (107 days' gestation), the clot of the *untreated wounds* was not longer present and the thickness of the newly formed epidermis was completely normalized (Figs. 3D and 4D). A more dense ECM network was formed. A general decrease in cell number was seen (Fig. 3D1 and D2 versus A2); myofibroblasts were only sporadically seen (Fig. 5D). At this time point more small as well as mature blood vessels were observed at the dermal side of the newly formed tissue (Fig. 3D2) compared to two weeks, however less blood vessels than in the normal fetal dermis.

In the wounds treated with COL, the clot was still present (Fig. 3E). The thickness of the newly formed epidermal layer was not normalized (Fig. 4E), but the wound area was completely covered by the epidermis at this time point. Single cells were present between the collagen bundles of the entire scaffold (Fig. 3E2) and numbers of α-SMA-positive cells were even decreased compared to the earlier time point (Fig. 5E versus B). Most importantly, a newly formed ECM layer was present between the epidermis (Fig. 3E and E1) and the scaffold which was devoid of myofibroblasts (Fig. 5E) and in which several blood vessels were formed, comparable to the appearance of the normal dermis. Only a few mature blood vessels were formed in the scaffold as revealed by a collagen IV staining (Fig. 6A).

In the wounds treated with COL-HEP/VF the clot was also still present. The newly formed epidermis was still hypertrophic with an irregular shape (Fig. 4F). ECM formation was mostly observed at the epidermal side of the scaffold (Fig. 3F1) and contained a decreased amount of myofibroblasts (Fig. 5F) compared to the earlier time point. In the scaffold further distal of the epidermis hardly any ECM formation was seen (Fig. 3F2). Compared to the bare COL implant, less cells, mainly α-SMA-negative (Fig. 5F), were present in the scaffold (Fig. 3F2 versus E2), but a similar amount of blood vessels was present in the scaffold (Fig. 6B versus A).

Eight weeks after surgery (140 days' gestation), the *untreated wound* had completely lost its clot. The granulation tissue was entirely replaced by ECM and had a density comparable with the normal dermis (Fig. 3G). There were no skin appendages in the newly formed tissue (Fig. 4G) and myofibroblasts were absent (Fig. 5G). A comparable amount of mature blood vessels was present in this newly formed ECM (Fig. 3G) when compared to the normal fetal dermis.

In the wounds treated with COL, the clot was also lost, whereas still parts of the epidermis were thickened (Fig. 3H). Interestingly, the entire scaffold was degraded and replaced by ECM (Fig. 3H). A decreased amount of myofibroblasts was seen compared to four weeks (Fig. 5E versus H). A higher amount of blood vessels was present throughout the newly formed ECM layer (Figs. 3H1, H2 and 6C) compared to the normal dermis.

In contrast, in the wounds treated with COL-HEP/VF part of the clot was still present. The thickness of the epidermal layer had decreased (Figs. 3I and 4I), but was still thicker than the newly formed epidermis of the untreated and the COL treated wound. Remarkably, some of the skin appendages of the epidermis were formed in the newly formed ECM (Figs. 3I1 and 4I). This ECM layer was not as dense as the newly formed ECM in the untreated and the COL treated wound. In contrast to the latter, a considerable part of the scaffold was still present (Fig. 3I). Although it still concerned low numbers, a higher influx of cells was seen in the scaffold at this time point compared to four weeks after treatment (Fig. 3I2 versus F2). The amount of myofibroblasts was decreased compared to the four week time point (Fig. 5I versus F). Besides mature blood vessels, many capillaries were formed in the scaffold (Fig. 6D and D1).

4. Discussion

Fetal tissue engineering has been proposed as a new concept in the surgical reconstruction of birth defects in the fetal period [25]. However, despite being a promising concept, hardly any studies have been published to tackle the various steps needed to establish a proof-of-concept. In this study we investigated whether biodegradable scaffolds with or without growth factors can be used to treat full-thickness fetal skin defects which facilitate epidermal overgrowth and dermal repair. We studied the healing of these skin defects by use of a bare collagen type I (COL) scaffold, a heparinised COL scaffold loaded with VEGF and FGF2 (COL-HEP/VF), or left untreated (no scaffold). We hypothesized that the pro-angiogenic growth factors VEGF and FGF2 might enhance vascularization and epithelialization, leading to improved wound healing.

The study showed that at term (8 weeks post surgery) proper epidermal layers were formed in all defects. Less wound contraction occurred in COL treated defects compared to untreated defects. Even less contraction was present in defects treated with COL-HEP/VF, but in contrast to COL treated defects, degradation of the scaffold was not completed at term. Concerning degradation of the scaffold, hardly or no macrophages infiltrated the COL and COL-HEP/VF scaffolds, suggesting that these cells did not play a role in fetal tissue engineering. Similar amounts or even less blood vessels were formed in the defects compared to the developing fetal dermis, with exception of COL-HEP/VF treated defects at term, showing excessive formation of capillaries in the scaffold. Overall, myofibroblasts were involved in the remodeling of the tissue, i.e. ECM formation and wound contraction.

It is highly important that wound contraction and scar formation will be minimized after fetal skin defects, as the fetus grows rapidly. Therefore we investigated the formation of ECM and the amount of contraction in time. Previously, a fetal sheep model has shown that the transition period from scarless to healing with scar formation in sheep occurs between 100 and 120 days [3]. However, fetal skin repair is not only dependant on gestational age, but also on the size of the defect. Wounds in mid-gestation fetal lambs of 2–4 mm heal without scarring, whereas wounds of 6–10 mm heal with formation of a scar [3]. In our study, wounds of 12 mm were made at 79 days of gestation. It was expected that the untreated wounds would heal with scar formation due to the size of the wound. Indeed, all untreated defects showed healing with scar formation and contraction. However, clearly less wound contraction was observed with COL treatment. Myofibroblasts have contractile characteristics in an attempt to close the wound. Another function of myofibroblasts is the production of new ECM components. A comparable amount of myofibroblasts was seen at two weeks post surgery in untreated and COL treated wounds. At 4 and 8 weeks myofibroblasts were still present in COL treated

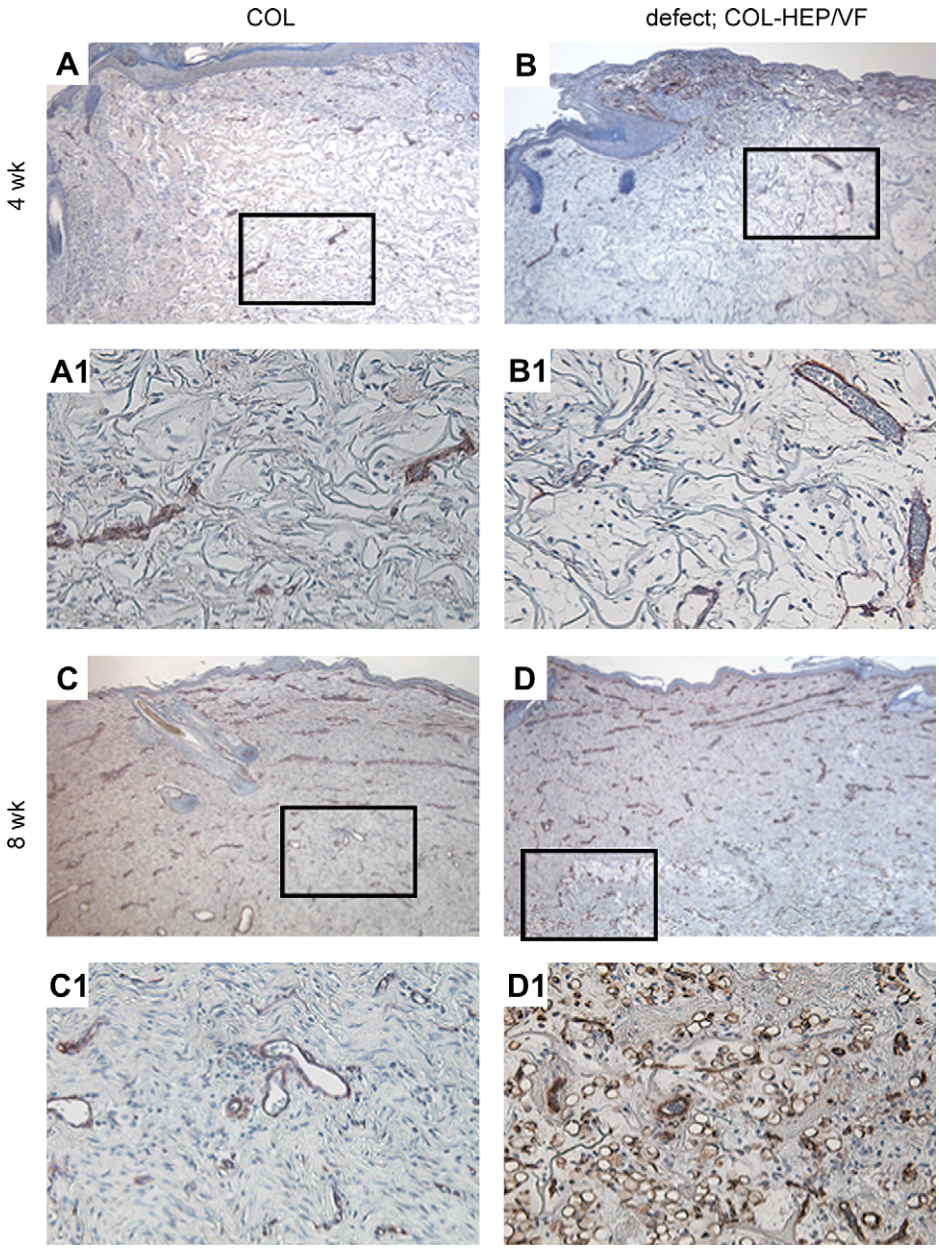

Fig. 6. Vascularization. Collagen IV staining of skin defects at different time points. Defect treated with COL at 4 weeks (A) and 8 weeks (C). Defect treated with COL-HEP/VF at 4 weeks (B) and 8 weeks (D). The boxed areas denote the corresponding region of higher magnification images. Original magnifications: 50× (A–E) and 200× (A1–E1).

wounds, resulting in a larger area of newly deposited ECM. As hypothesized, treatment of the skin defect with COL-HEP/VF diminished contraction even more. In accordance with this, fewer myofibroblasts were present. This is probably due to the incorporation of FGF2, because *in vitro* and *in vivo* studies have shown that FGF2 can inhibit and reverse the differentiation of fibroblasts to myofibroblasts [13,14,26,27].

Implantation of a biomaterial, like our degradable type I collagen scaffold, will induce an inflammatory response by the non-specific immune system, known as the foreign body reaction (FBR). In general the FBR will induce resorption of degradable scaffolds after implantation. Key players in the adult FBR are macrophages and giant cells. However, little is known about the FBR in fetal applications. It is known that in fetal wound healing less inflammation is induced compared to adult wound healing, which can be due to the fact that the innate immune system is less mature in the fetus. In the current fetal lamb model hardly any or no macrophages were detected in any of the histological specimens, and most of the cells were myofibroblasts. We wanted to confirm the scarcity of macrophages by a macrophage staining, but antibodies against sheep macrophages are not available. Several other macrophage antibodies have been tested to see if these cross-react, but none of these antibodies were successful. In accordance with the absence of macrophages, also giant cells (fused macrophages) were not present in the fetal skin wounds. This is a major difference with the adult situation in which implanted biodegradable scaffolds are finally phagocytosed by giant cells. In the current fetal model, COL and COL-HEP/VF scaffolds did degrade but as mentioned giant cells were not involved, suggesting that the scaffolds were degraded by enzymes secreted by (myo)fibroblasts.

In fetal tissue engineering it is important that a good balance exists between the degradation of the scaffold and new tissue

formation, i.e. epithelial overgrowth and proper dermal regeneration. We observed a faster tissue remodeling in the COL treated wounds compared to COL-HEP/VF treated defects. At four weeks in COL treated wounds, part of the collagen scaffold was degraded and replaced by an ECM layer that integrated with the original dermis. At eight weeks, the entire scaffold was degraded and replaced by new ECM. In contrast, in the COL-HEP/VF treated wounds, a large part of the scaffold was still present at 8 weeks post surgery, demonstrating that remodeling is still in progress. These differences between COL and COL-HEP/VF implicate that fetal TE can be influenced by growth factors leading to different degradation patterns.

Another major difference between COL and COL-HEP/VF treated defects was the hyperplasia of the epidermis observed at 2 and 4 weeks post surgery in COL-HEP/VF treated wounds. This could be caused by FGF2 as well as VEGF. It is known that FGF2 can have a mitogenic effect on keratinocytes, thereby promoting epithelialization in adult wound healing [15,16]. VEGF can also stimulate the proliferation and migration of keratinocytes *in vitro* [28]. Furthermore, application of VEGF in a diabetic wound healing model showed accelerated wound healing with enhanced epithelialization [29]. However, finally at 8 weeks a proper epidermal layer has been formed. Furthermore, enhanced angiogenesis was observed in the COL-HEP/VF treated wounds. Both VEGF and FGF2 can promote angiogenesis and the combination of VEGF and FGF2 has been shown to have synergistic effects on neovascularization both *in vitro* and *in vivo* [9–12]. Although excessive formation of capillaries was observed in these scaffolds 8 weeks post surgery, we do not know whether these capillaries are functional, because erythrocytes were not observed in these capillaries.

A highly interesting observation is the formation of new appendages in the wounded area of the COL-HEP/VF treated wounds 8 weeks after surgery. Regeneration of these specialized structures indicates an enhanced functional healing. These newly formed appendages were less mature (smaller compared to appendages in the normal skin at this time of development) than the appendages in the unwounded skin, indicating that the appendages have not migrated from the wound edges.

For optimal binding of growth factors to the scaffold, the scaffolds were heparinised. We have to realize that directly after implantation the scaffold is in contact with the amniotic fluid. It is known that several growth factors are present in the amniotic fluid, like hepatocyte growth factor (HGF), insulin-like growth factor (IGF), FGF2, and VEGF. We can not exclude that, in addition to the loaded growth factors, also growth factors from the wound site or from the amniotic fluid bound to the heparin in COL-HEP/VF, leading to a long-term effect of these growth factors.

For future tissue engineering approaches of congenital defects such as spina bifida, scaffolds could be useful for wound closure. *In utero* coverage of the defect with a scaffold will shorten the exposure time of the spinal cord to the amniotic fluid, which will likely improve the neurologic outcome by preventing further damage. However, future studies will be needed to investigate if the addition of growth factors is beneficial in the case of spina bifida.

5. Conclusion

The evaluation of biomaterials for specific applications should be evaluated in model systems resembling the clinical situation. This study showed that tissue engineering *in utero* is a promising method in treatment of full-thickness fetal skin defects. Both COL and COL-HEP/VF treated wounds showed a proper re-epithelialization and healing without a (chronic) FBR. COL treated wounds show less contraction than untreated wounds and this effect was even enhanced in COL-HEP/VF. Furthermore, the addition of these growth factors leads to an increased angiogenesis and to regeneration of the skin appendages.

Acknowledgements

We gratefully acknowledge C.N. Verrijp (Department of Pathology, Radboud University Nijmegen Medical Centre) and M.G.J. Sommers, A.E.J. Hanssen, C. van den Broek, L. Ennen (Central Animal Laboratory, Radboud University Nijmegen Medical Centre) and B. Kortmann (Pediatric Urology, Radboud University Nijmegen Medical Centre) for their contributions to this study. This work was supported by EU-FP6 project EuroSTEC (soft tissue engineering for congenital birth defects in children; LSHB-CT-2006-037409) and 'Agiko stipendium' from 'The Netherlands Organization for Health Research and Development' and Radboud University Nijmegen Medical Centre, The Netherlands, project number 920-03-456.

References

[1] Heffez DS, Aryanpur J, Hutchins GM, Freeman JM. The paralysis associated with myelomeningocele: clinical and experimental data implicating a preventable spinal cord injury. Neurosurgery 1990;26:987–92.
[2] Bullard KM, Longaker MT, Lorenz HP. Fetal wound healing: current biology. World J Surg 2003;27:54–61.
[3] Cass DL, Bullard KM, Sylvester KG, Yang EY, Longaker MT, Adzick NS. Wound size and gestational age modulate scar formation in fetal wound repair. J Pediatr Surg 1997;32:411–5.
[4] Daamen WF, Nillesen STM, Hafmans T, Veerkamp JH, van Luyn MJA, van Kuppevelt TH. Tissue response of defined collagen–elastin scaffolds in young and adult rats with special attention to calcification. Biomaterials 2005;26:81–92.
[5] Eggink AJ, Roelofs LA, Feitz WF, Wijnen RM, Mullaart RA, Grotenhuis JA, et al. In utero repair of an experimental neural tube defect in a chronic sheep model using biomatrices. Fetal Diagn Ther 2005;20:335–40.
[6] Eggink AJ, Roelofs LA, Lammens MM, Feitz WF, Wijnen RM, Mullaart RA, et al. Histological evaluation of acute covering of an experimental neural tube defect with biomatrices in fetal sheep. Fetal Diagn Ther 2006;21:210–6.
[7] Eggink AJ, Roelofs LA, Feitz WF, Wijnen RM, Lammens MM, Mullaart RA, et al. Delayed intrauterine repair of an experimental spina bifida with a collagen biomatrix. Pediatr Neurosurg 2008;44:29–35.
[8] Ferrara N. VEGF: an update on biological and therapeutic aspects. Curr Opin Biotechnol 2000;11:617–24.
[9] Pepper MS, Ferrara N, Orci L, Montesano R. Potent synergism between vascular endothelial growth factor and basic fibroblast growth factor in the induction of angiogenesis in vitro. Biochem Biophys Res Commun 1992;189:824–31.
[10] Asahara T, Bauters C, Zheng LP, Takeshita S, Bunting S, Ferrara N, et al. Synergistic effect of vascular endothelial growth factor and basic fibroblast growth factor on angiogenesis in vivo. Circulation 1995;92:II365–71.
[11] Lee KY, Peters MC, Mooney DJ. Comparison of vascular endothelial growth factor and basic fibroblast growth factor on angiogenesis in SCID mice. J Control Release 2003;87:49–56.
[12] Nillesen STM, Geutjes PJ, Wismans R, Schalkwijk J, Daamen WF, van Kuppevelt TH. Increased angiogenesis and blood vessel maturation in acellular collagen–heparin scaffolds containing both FGF2 and VEGF. Biomaterials 2007;28:1123–31.
[13] Ono I, Akasaka Y, Kikuchi R, Sakemoto A, Kamiya T, Yamashita T, et al. Basic fibroblast growth factor reduces scar formation in acute incisional wounds. Wound Repair Regen 2007;15:617–23.
[14] Ono I, Tateshita T, Inoue M. Effects of a collagen matrix containing basic fibroblast growth factor on wound contraction. J Biomed Mater Res 1999;48:621–30.
[15] Hebda PA, Klingbeil CK, Abraham JA, Fiddes JC. Basic fibroblast growth factor stimulation of epidermal wound healing in pigs. J Invest Dermatol 1990;95:626–31.
[16] Sogabe Y, Abe M, Yokoyama Y, Ishikawa O. Basic fibroblast growth factor stimulates human keratinocyte motility by Rac activation. Wound Repair Regen 2006;14:457–62.
[17] Geutjes PJ, Daamen WF, Buma P, Feitz WF, Faraj KA, van Kuppevelt TH. From molecules to matrix: construction and evaluation of molecularly defined bioscaffolds. Adv Exp Med Biol 2006;585:279–95.
[18] Pieper JS, Oosterhof A, Dijkstra PJ, Veerkamp JH, van Kuppevelt TH. Preparation and characterization of porous cross-linked collagenous matrices containing bioavailable chondroitin sulphate. Biomaterials 1999;20:847–58.
[19] Gilbert DL, Kim SW. Macromolecular release from collagen monolithic devices. J Biomed Mater Res 1990;24:1221–39.
[20] Olde Damink LHH, Dijkstra PJ, van Luyn MJA, van Wachem PB, Nieuwenhuis P, Feijen J. Cross-linking of dermal sheep collagen using a water-soluble carbodiimide. Biomaterials 1996;17:765–73.

[21] Elson LA, Morgan WT. A colorimetric method for the determination of glucosamine and chondrosamine. Biochem J 1933;27:1824–8.
[22] Yannas IV, Burke JF, Gordon PL, Huang C, Rubenstein RH. Design of an artificial skin. II. Control of chemical composition. J Biomed Mater Res 1980;14:107–32.
[23] Smits NC, Robbesom AA, Versteeg EMM, van de Westerlo EMA, Dekhuijzen PNR, van Kuppevelt TH. Heterogeneity of heparan sulfates in human lung. Am J Respir Cell Mol Biol 2004;30:166–73.
[24] van Kuppevelt TH, Dennissen MA, van Venrooij WJ, Hoet RM, Veerkamp JH. Generation and application of type-specific anti-heparan sulfate antibodies using phage display technology. Further evidence for heparan sulfate heterogeneity in the kidney. J Biol Chem 1998;273:12960–6.
[25] Kunisaki SM, Armant M, Kao GS, Stevenson K, Kim H, Fauza DO. Tissue engineering from human mesenchymal amniocytes: a prelude to clinical trials. J Pediatr Surg 2007;42:974–9.
[26] Maltseva O, Folger P, Zekaria D, Petridou S, Masur SK. Fibroblast growth factor reversal of the corneal myofibroblast phenotype. Invest Ophthalmol Vis Sci 2001;42:2490–5.
[27] Ishiguro S, Akasaka Y, Kiguchi H, Suzuki T, Imaizumi R, Ishikawa Y, et al. Basic fibroblast growth factor induces down-regulation of alpha-smooth muscle actin and reduction of myofibroblast areas in open skin wounds. Wound Repair Regen 2009;17:617–25.
[28] Wilgus TA, Matthies AM, Radek KA, Dovi JV, Burns AL, Shankar R, et al. Novel function for vascular endothelial growth factor receptor-1 on epidermal keratinocytes. Am J Pathol 2005;167:1257–66.
[29] Brem H, Kodra A, Golinko MS, Entero H, Stojadinovic O, Wang VM, et al. Mechanism of sustained release of vascular endothelial growth factor in accelerating experimental diabetic healing. J Invest Dermatol 2009;129:2275–87.